Microsc. Microanal. Microstruct. **3** (1992) 471–482 DECEMBER **1992**, PAGE 471

Classification
Physics Abstracts
07.80 — 68.48 — 81.30

Atom-probe and TEM study of the isothermal ω and secondary α phases in a Ti −10 V −2 Fe −3 Al alloy

L. Hadjadj([1]), M.H. Campagnac([2,3]), A. Vassel([2]) and A. Menand([1])

([1]) Laboratoire de Microscopie Ionique, URA CNRS 808, Faculté des Sciences, BP 118, 76134 Mt St Aignan cedex, France

([2]) Office National d'Etudes et de Recherches Aérospatiales, 92322 Chatillon cedex, France

([3]) Aérospatiale, BP 76, 92152 Suresne, France

(Received 25 September 1992, accepted 21 January 1993)

Résumé. — La décomposition de la matrice β de l'alliage Ti-10 V-2 Fe-3 Al lors de vieillissements à 573 K est étudiée par Microscopie Electronique à Transmission et Sonde Atomique. La combinaison des 2 techniques permet de suivre la formation et l'évolution de la phase ω isotherme ainsi que la précipitation de la phase α secondaire. Les résultats obtenus conduisent à décrire la décomposition de la matrice β par un processus non classique en deux étapes.

Abstract. — The decomposition of the β matrix in the Ti-10 V-2 Fe-3 Al alloy during aging at 573 K is studied by TEM and Atom Probe. The combination of the two techniques allows to follow the formation and the evolution of the isothermal ω phase as well as the precipitation of the secondary α phase. The β matrix decomposition is described as a two stage process.

1. Introduction.

Titanium base alloys have low density and high mechanical strength. For these reasons they are used is many domains of modern industry, particularly in aerospace applications. The Ti-10 V-2 Fe-3 Al alloy is a β metastable alloy designed for making structural components of aircrafts.

After a solution heat treatment in the $(\alpha + \beta)$ field and quenching the Ti-10wt% V-2wt% Fe-3wt% Al alloy is composed of β grains and a low volume fraction of residual primary α phase at β grain boundaries (Fig. 1).

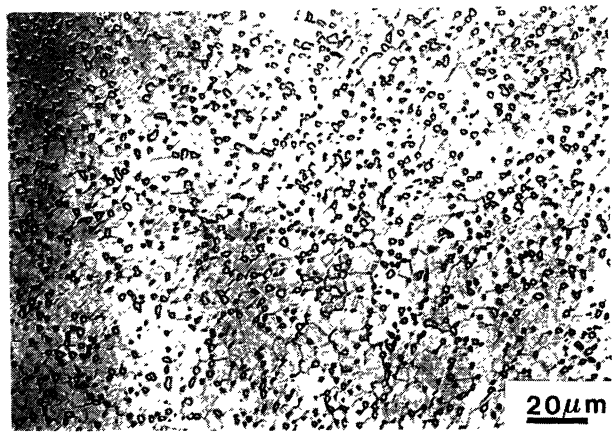

Fig. 1. — Optical micrograph of a sample in the as quenched state.

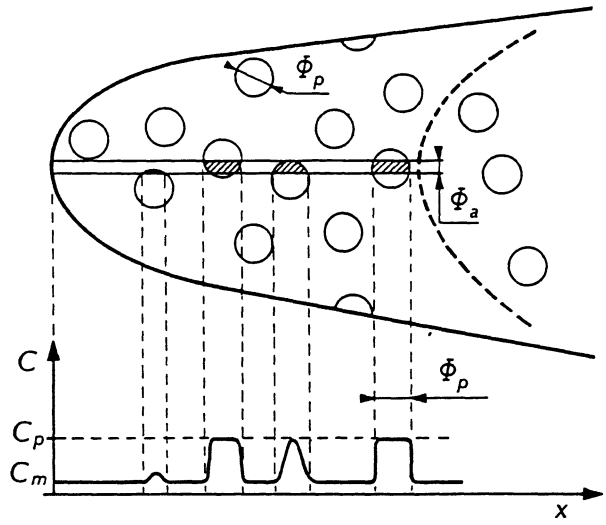

Fig. 2. — Atom Probe microanalysis of a two phase material with particles of diameter Φ_p. The diameter Φ_a of the analysis cylinder gives the lateral resolution. The composition profiles may be drawn for each element as a function of analysed depth. C_p is the precipitate concentration and C_m the matrix one.

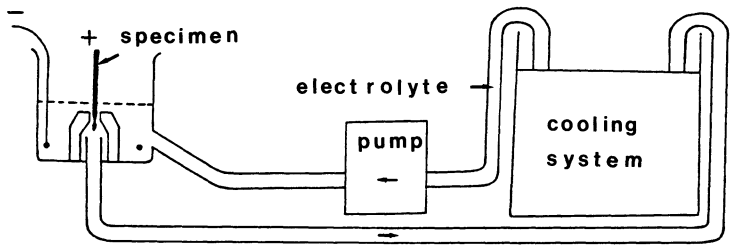

Fig. 3. — Schematic diagram of the electropolishing device used for tip preparation when the material is strongly subjected to oxydation.

The purpose of this study is to report a combined Atom-Probe (AP) and TEM study of the decomposition of the β matrix during thermal aging.

2. Experimental.

The alloys were supplied by CEZUS compagny, heat treatments and TEM observations were performed at the Office National d'Etudes et de Recherches Aerospatiales (ONERA) [1].

The alloys were solution treated at 1053 K for 2 hours in the $\alpha+\beta$ field, just below the β transus, and water quenched. Aging treatments were performed at 573 K for increasing times: 15 mn, 1 h, 8 h, 240 h and 1 000 h.

The atom-probe techniques have been described in details elsewhere [2-4]. The instrument consists essentially in two parts: a Field Ion Microscope (FIM) which allows the sample surface to be observed with a spatial resolution close to an atomic scale, and a time of flight mass spectrometer which gives an atom by atom analysis of the sample.

Schematically (Fig. 2), atom probe investigation of a material may be interpreted as the analysis of the specimen along a cylinder. The lateral resolution Φ_a is chosen between 0.5 nm and 5 nm whereas the depth resolution is strictly equal to one atomic plane.

The APFIM specimens were prepared as sharpened needles by anodic electropolishing in a solution of 6 % perchloric acid 34 % n-butylacohol and 60 % methanol, cooled at 233 K. In order to prevent passivation phenomena, a circulation of the electrolyte is produced by means of a peristaltic pump (Fig. 3).

The difficulties to overcome these passivation problems in tip preparation probably explain that no Atom Probe study was reported in titanium base alloys before our first works in 1986 [5, 6].

AP reliable data were obtained by using a pulse fraction of 20 % of the DC voltage and a tip temperature between 40 K and 50 K. Analyses were carried out in the range 10^{-10} to 10^{-9} Torr [7].

3. Results.

The mass spectrum shown in figure 4 indicates that all the elements are detected as doubly charged ions and are unambiguously identified.

3.1 AS QUENCHED STATE. — The optical micrograph of figure 1 reveals a residual primary α phase at β grain boundaries. The size of α grains is about 1 micron whereas the β precipitates are about 10 microns in size. This allows electron microprobe analyses to be performed. The results are compared to those obtained by atom probe analysis in table I. The good agreement between the results obtained by both techniques points out the reliability of AP for titanium base alloy investigation.

TEM observations inside β grains reveal the presence of a fine precipitation (a few nm in size). These particles are identified by microdiffraction (Fig. 5) as athermal ω precipitates.

The ω precipitates are uniformly distributed within the β grains and no α phase precipitation is detected. The athermal ω precipitates are formed by a displacement mechanism [8] without composition change (Fig. 6).

The composition profiles obtained by AP analysis (Fig. 7) do not show any composition heterogeneity expect the statistical sampling fluctuations and therefore indicate that the chemical composition of the β grains in the as quenched state is homogeneous.

Table I. — *Composition (at%) of β and primary α phases as obtained by electron microprobe and atom probe.*

		Ti	V	Fe	Al
β	Atom Probe	82.9 ± 0.4	10.3 ± 0.3	2.05 ± 0.15	4.75 ± 0.2
	Electron Microprobe	82.20	10.45	1.84	5.51
primary α	Atom Probe	87.6 ± 0.6	3.2 ± 0.3	0.3 ± 0.1	8.9 ± 0.5
	Electron Microprobe	88.16	3.50	0.19	8.15

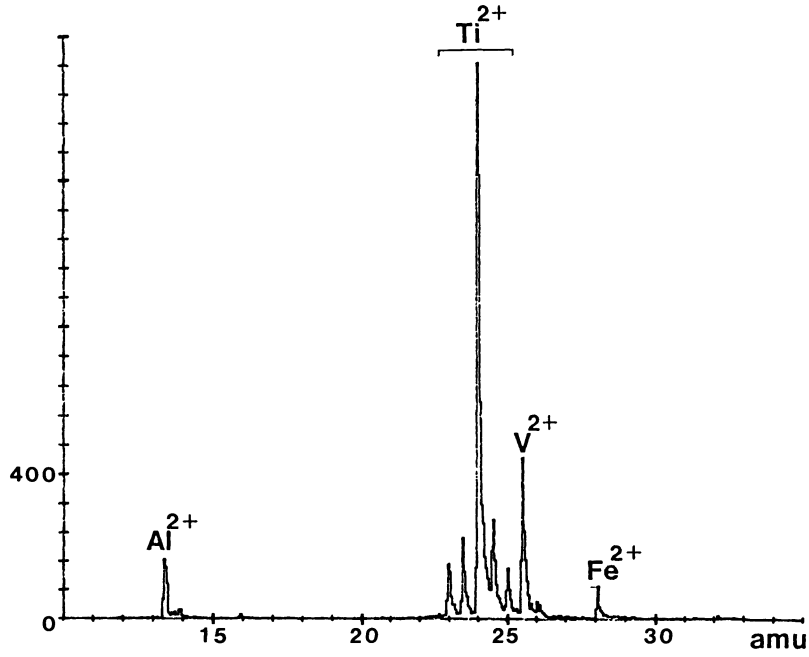

Fig. 4. — Atom Probe mass spectrum of a Ti-10 V-2 Fe-3 Al alloy.

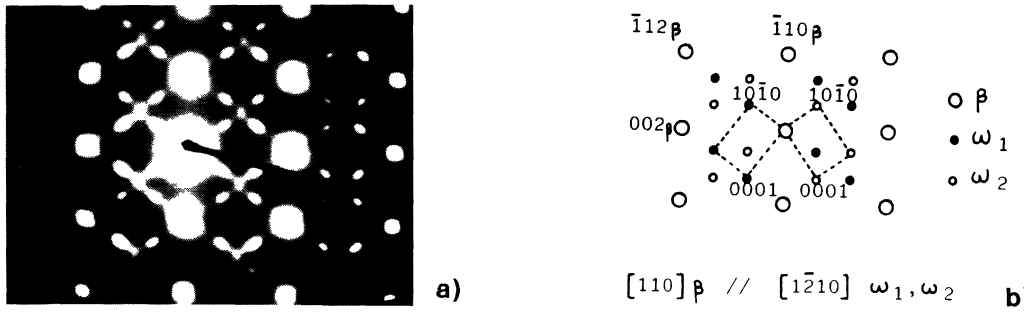

Fig. 5. — Electron diffraction pattern (a) and indexation (b) related to the athermal ω phase for a sample in the as quenched state.

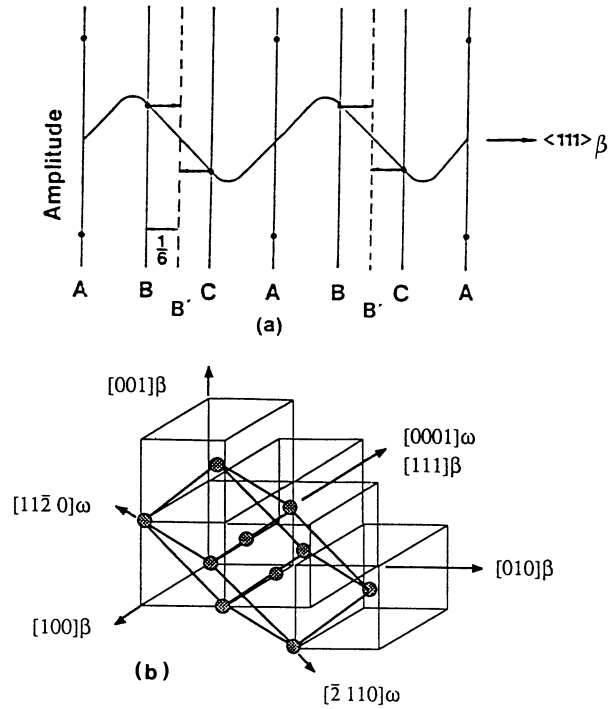

Fig. 6. — Schematic representation of the diffusionless mechanism of the $\beta \rightarrow \omega$ transformation. (a) (111) planes on edge showing bcc stacking sequence ABC ABC. The collapsing of two neighboring (111) planes out of three produces an hexagonal stacking sequence AB' AB'. (b) perspective view of β and ω cells with the orientation relationships deduce from the mechanism previously described: [0001] ω // [111] β and $[11\bar{2}0]$ ω // [110] β.

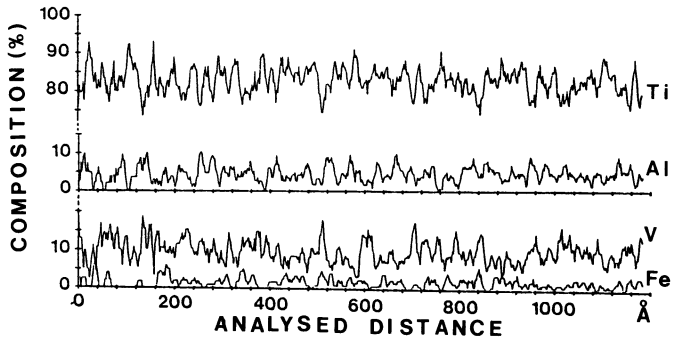

Fig. 7. — AP composition profiles of a sample in the as quenched state.

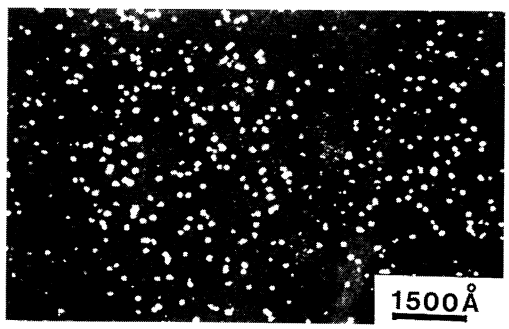

Fig. 8. — Dark field electron micrograph of a sample aged 15 mn at 573 K.

3.2 ALLOY AGED 15 mn AT 573 K. — Figure 8 shows a dark field electron micrograph of an alloy aged 15 mn at 573 K. The micrograph exhibits the presence of small isothermal ω phase precipitates the size of which is close to 10 nm. However, the AP composition profiles (Fig. 9) do not reveal any noticeable composition heterogeneity. Of course, the possibility that we systematically missed the ω particles during AP analysis has to be considered. But the fact that we obtained the same compositions for the as quenched and 15 mn aged conditions (Tab. II), compositions which are also in good agreement with those obtained by microprobe analysis, leads us to think that our analyses are actually representative of the β grain composition which is indeed homogeneous. Also we must say that these analyses represent a total probe depth of 700 nm through the β matrix which gives obviously a very great probability for the particles to be crossed by the analysis cylinder.

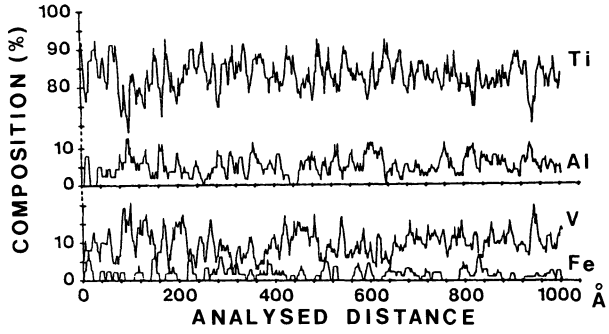

Fig. 9. — AP composition profiles of a sample aged 15 mn at 573 K.

Table II. — *Overall composition (at%) of the β grains as deduced from atom probe data for the as-quenched and 15 mn aged conditions, compared to the composition obtained by electron microprobe analysis.*

	Ti	V	Fe	Al
15 mn	82.6 ± 0.3	10.4 ± 0.2	2.0 ± 0.1	5.0 ± 0.2
as quenched	82.9 ± 0.4	10.3 ± 0.3	2.0 ± 0.1	4.8 ± 0.2
microprobe	82.20	10.45	1.84	5.51

3.3 ALLOYS AGED 1 h AND 8 h AT 573 K. — As shown by TEM examination (Fig. 10), the isothermal ω precipitates reach 15 nm in size for 1 h aging time and 20 nm for 8 h. The AP composition profiles (Fig. 11) are completely different from those previously shown for a 15 mn aging time. Large titanium rich zones are now clearly visible and they are interpreted as the crossing of isothermal ω phase precipitates by the analysis cylinder [9].

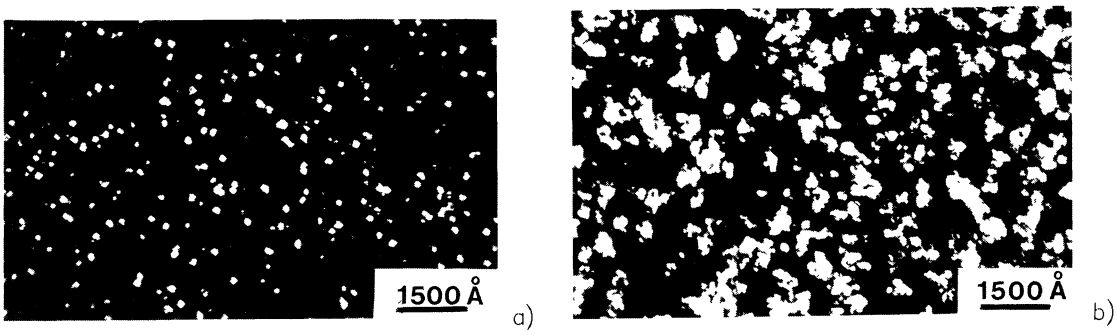

Fig. 10. — Dark field electron micrograph of a sample aged at 573 K for: a) 1 h; b) 8 h.

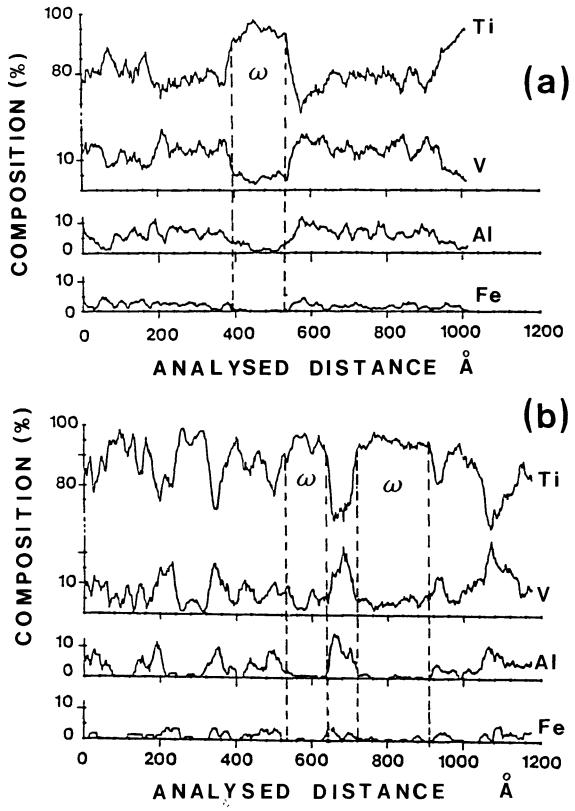

Fig. 11. — Atom probe composition profiles of sample aged at 573 K for: a) 1 h; b) 8 h.

These precipitates are depleted in all alloying elements alpha (Al) and beta (V, Fe) stabilizers.

After a 1 hour aging, the atomic fraction deduced from the composition is $F_a = 20\ \% \pm 5\ \%$ which gives a volume fraction $F_v = 21\ \% \pm 5\ \%$. For a 8 hour aging the volume fraction increases and reaches $39\ \% \pm 5\ \%$.

For these two aging times a statistical treatment of the concentration profiles [10, 11] reveals the existence of aluminium enriched zones in the β matrix.

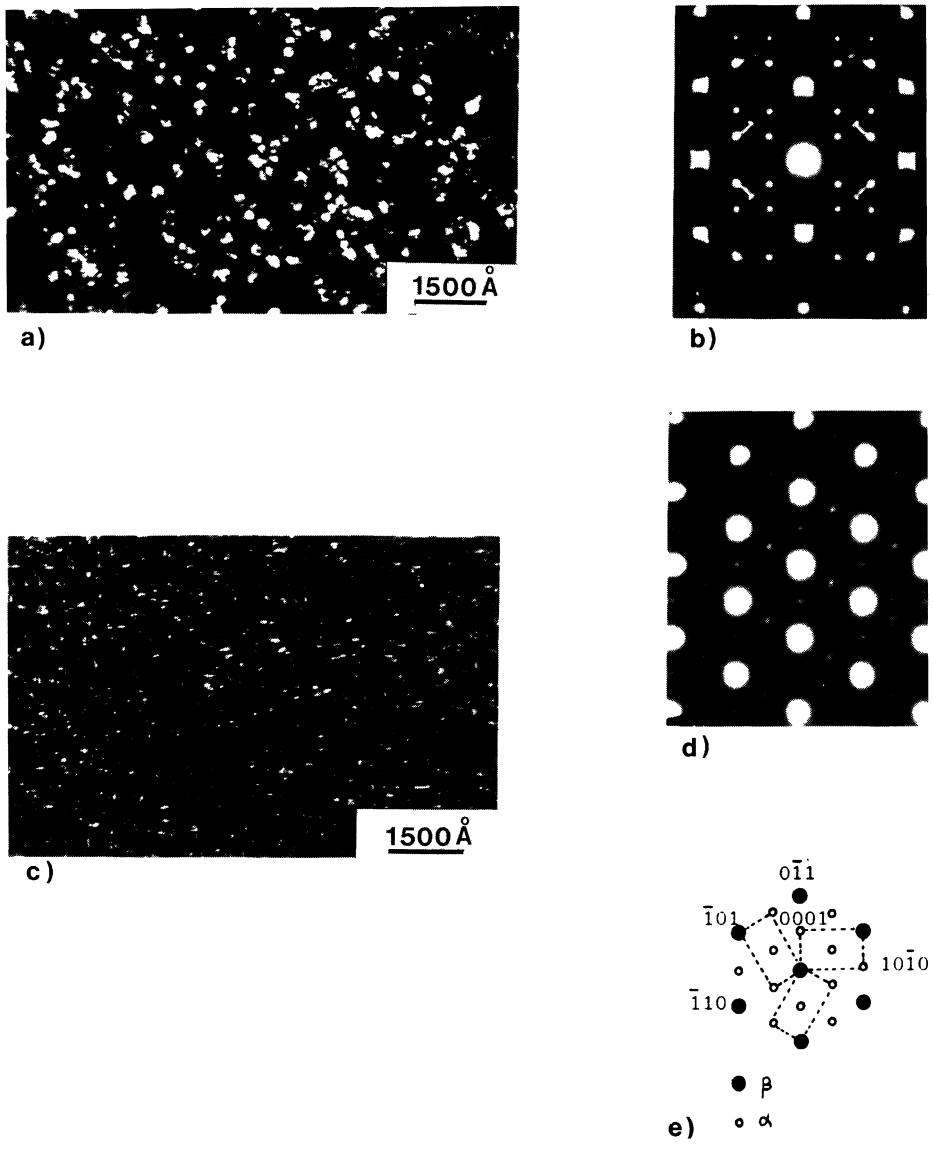

Fig. 12. — TEM examination of a sample aged 240 h at 573 K. a) Dark field observation of the isothermal ω phase. b) Electron diffraction pattern $\langle 110 \rangle$ β. c) Dark field observation of the secondary α phase. d) Electron diffraction pattern $\langle 111 \rangle$ β. e) Indexation of d) [111] β // [1210] α.

3.4 ALLOYS AGED 240 h AND 1 000 h AT 573 K. — For these aging times the TEM observations (Fig. 12) indicate an increase for the ω precipitate size (25 nm) and reveal the existence of a very fine needle-shaped α phase precipitation. This secondary α phase seems to nucleate preferentially at β-ω interfaces [1].

The composition profiles (Fig. 13) are now much more complex. In addition to the large titanium rich zones (ω precipitates) seen in the previous treatments, some aluminium enriched zones are now visible. They are interpreted as the crossing of α needles by the analysis cylinder.

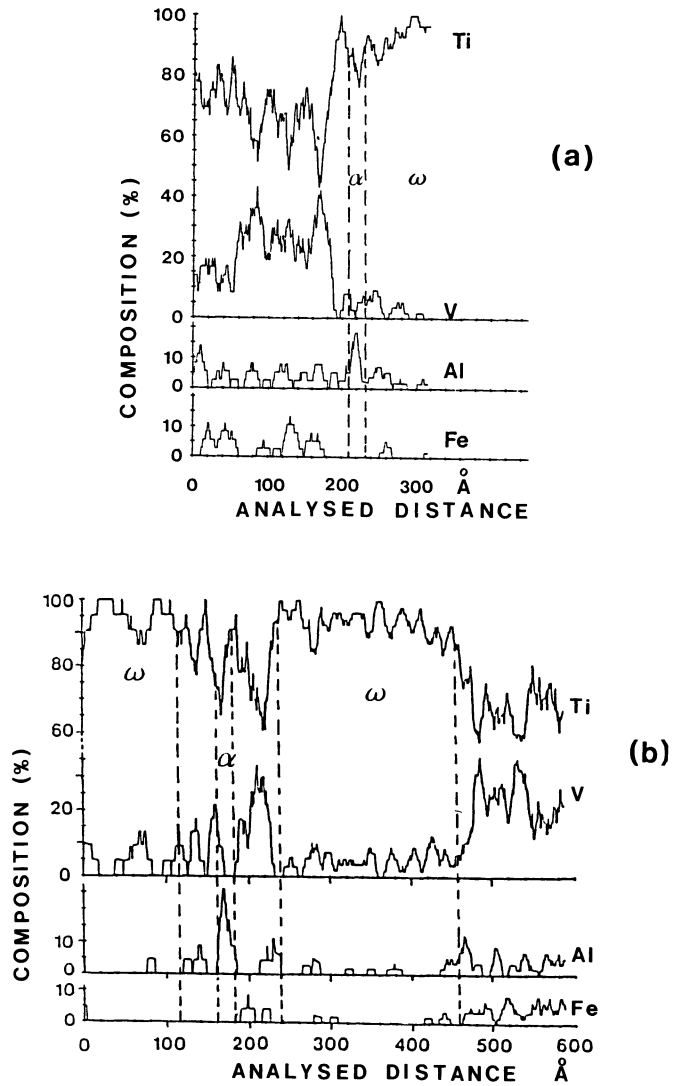

Fig. 13. — AP composition profiles of samples aged at 573 K; a) 240 h; b) 1000 h.

4. Discussions.

Table III summarizes the observed composition and volume fraction values related to the β, ω and α phases for the different aging times.

Table III. — *Composition (at%) and volume fraction of the β, ω, and secondary α phases as deduced from atom probe data for different aging times at 573 K.*

		Ti	V	Fe	Al	F_v %
1 h	matrix β	79.8 ± 0.8	12.2 ± 0.3	2.3 ± 0.2	5.7 ± 0.2	
1 h	ω	92.5 ± 0.6	4.6 ± 0.5	0.9 ± 0.2	2.0 ± 0.3	21 %
8 h	matrix β	74.7 ± 0.7	15.8 ± 0.6	2.3 ± 0.2	7.2 ± 0.4	
8 h	ω	93.1 ± 0.5	4.6 ± 0.4	0.7 ± 0.2	1.6 ± 0.2	39 %
240 h	matrix β	67.9 ± 1.0	23.2 ± 0.9	4.3 ± 0.5	4.6 ± 0.5	
240 h	ω	94.0 ± 0.3	3.7 ± 0.3	0.9 ± 0.1	1.4 ± 0.2	51.4 %
240 h	secondary α	87.1 ± 1.3	3.6 ± 0.7	0.6 ± 0.3	8.7 ± 1.1	10.7 %
1 000 h	matrix β	68.2 ± 0.7	22.7 ± 0.6	4.4 ± 0.3	4.7 ± 0.3	
1 000 h	ω	92.7 ± 0.4	4.5 ± 0.3	0.65 ± 0.1	2.15 ± 0.2	48 %
1 000 h	secondary α	86.9 ± 0.9	3.45 ± 0.5	0.8 ± 0.2	8.85 ± 0.7	13.7 %

Another synthetic way to follow the decomposition of the β matrix is to use the differential distribution [11] of titanium and aluminium. These histograms give the difference between the experimental concentration distribution and a statistical frequency distribution, which can be accounted for by a binomial distribution for a random solid solution.

As the isothermal ω phase is a titanium rich phase the differential distribution of titanium describes the ω phase evolution whereas the aluminium differential distribution allows to follow the α aluminium enriched phase precipitation.

Figure 14 displays the two sets of differential distributions for aluminium (left part) and titanium (right part) obtained for the different aging times. Each curve is calculated from concentration profiles corresponding to more than 50 000 atoms.

These results lead us to describe the decomposition of the β matrix for the Ti-10 V-2 Fe-3 Al alloy as follows: after quenching the alloy is chemically homogeneous but structurally decomposed into two phases, the β matrix (BCC) and the hexagonal metastable athermal ω phase. During aging the isothermal ω phase which appears, proceeds in a two stage process. In a first stage particles grow by a displacement méchanism similar to the one responsible for the athermal ω phase formation and without detectable composition change. In a second stage ($t > 15$ mn at 573 K) the isothermal precipitates grow through a long range diffusion mechanism. This two stage process is in good agreement with the model proposed by Duerig [12] and Fatemi [13] in contrast with a classical diffusional nucleation and growth mode.

The titanium enrichment of the ω particles and the correlated aluminium rejection during the second stage favour the secondary α phase precipitation which therefore appears when the composition change of the ω phase occurs.

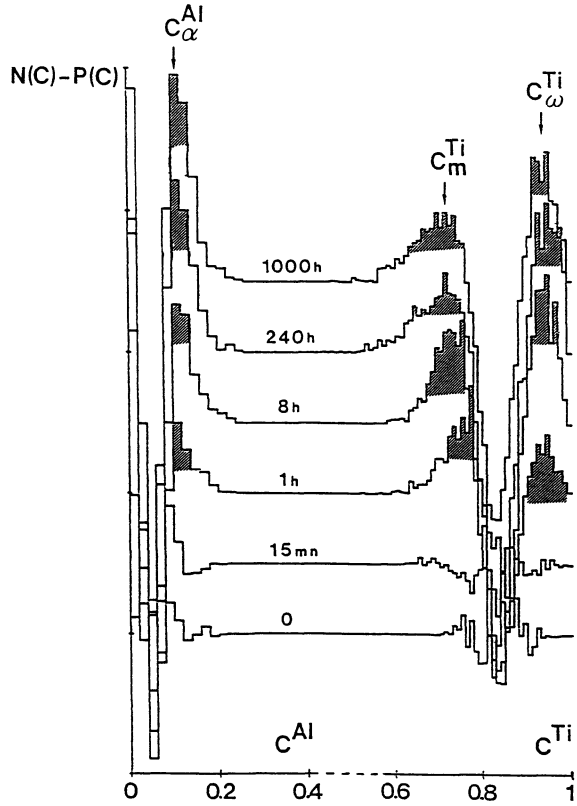

Fig. 14. — Differential distributions related to aluminium (left part) and titanium (right part) as a function of aging time at 573 K.

The composition change of ω particles also produces a misfit between the matrix and precipitate lattices. The β - ω misfit becomes more pronounced as the β matrix is enriched in the alloying elements. As a result, the β/ω interface discontinuities may provide preferential nucleation sites for the secondary α phase.

5. Conclusion.

A combined TEM and AP study allowed us to describe the ω and α phase formation in a Ti-10 V-2 Fe-3 Al alloy. The isothermal ω phase forms and first grows by a displacement mechanism without major composition change and then grows in a second stage by a diffusion process with the rejection of all the alloying elements (Al, Fe, V). The secondary α phase forms at β/ω interfaces when the ω composition change occurs, consuming the aluminium rejected by the ω phase.

Acknowledgements.

These researches were for a part financially supported by the Direction des Recherches et Etudes Techniques (DRET) we would like to thank (Contract n°87/031).

References

[1] CAMPAGNAC M.H., Thèse de doctorat, Université P. et M. Curie, Paris (1988).
[2] BLAVETTE D. and MENAND A., *Ann. Chimie* **11** (1986) 321-384.
[3] MILLER M.K. and SMITH G.D.W., Atom probe microanalysis principles and applications to materials problems (Mat. Res. Soc., 1989).
[4] BLAVETTE D. and AUGER P., *Microsc. Microanal. Microstruct.* **1** (1990) 481.
[5] MENAND A., CHAMBRELAND S. and MARTIN C., *J. Phys. Colloq. France* **47** (1986) C2-197.
[6] MENAND A., HADJADJ L. and VASSEL A., *Scr. Met.* **21** (1987) 1295.
[7] HADJADJ L., Thèse de Doctorat, Université de Rouen (1988).
[8] WILLIAMS J.C., De FONTAINE D. and PATRON N.E., *Met. Trans.* **4** (1973) 2701.
[9] MENAND A., HADJADJ L. and BLAVETTE D., Proc. of "6th world conferance on titanium" Les Editions de Physique (1988) p.1577.
[10] BLAVETTE D., GRANCHER G. and BOSTEL A., *J. Phys. Colloq. France* **49** (1988) C6-433.
[11] AUGER P., MENAND A. and BLAVETTE D., *J. Phys. Colloq. France* **49** (1988) C6-439.
[12] DUERIG T.W., TERLINDE G.T. and WILLIAMS J.C., *Met. Trans.* **11A** (1980) 1987.
[13] FATEMI M., *Philos. Mag.* **A50** (1984) 711.